Differential Effects of Temperature and Hydrostatic Pressure on the Formation of Quinonoid Intermediates from L-Trp and L-Met by H463F Mutant *Escherichia coli* Tryptophan Indole-lyase†

Robert S. Phillips*,‡ and Georg Holtermann§

Departments of Chemistry and of Biochemistry and Molecular Biology, University of Georgia, Athens, Georgia 30602-2556, and Department of Physical Biochemistry, Max-Planck-Institut für Molekulare Physiologie, Otto-Hahn-Strasse 6, 44227 Dortmund, Germany

Received June 3, 2005; Revised Manuscript Received August 31, 2005

ABSTRACT: *Escherichia coli* tryptophan indole-lyase (Trpase) is a bacterial pyridoxal 5′-phosphate (PLP)-dependent enzyme which catalyzes the reversible β-elimination of L-Trp to give indole and ammonium pyruvate. H463F mutant *E. coli* Trpase (H463F Trpase) has very low activity with L-Trp, but it has near wild-type activity with other in vitro substrates, such as *S*-ethyl-L-cysteine and *S*-(*o*-nitrophenyl)-L-cysteine [Phillips, R. S., Johnson, N., and Kamath, A. V. (2002) Formation *in vitro* of Hybrid Dimers of H463F and Y74F Mutant *Escherichia coli* Tryptophan Indole-lyase Rescues Activity with L-Tryptophan, *Biochemistry 41*, 4012−4019]. The interaction of H463F Trpase with L-Trp and L-Met, a competitive inhibitor, has been investigated by rapid-scanning stopped-flow, high-pressure, and pressure jump spectrophotometry. Both L-Trp and L-Met bind to H463F Trpase to form equilibrating mixtures of external aldimine and quinonoid intermediates, absorbing at ∼420 and ∼505 nm, respectively. The apparent rate constant for quinonoid intermediate formation exhibits a hyperbolic dependence on L-Trp and L-Met concentration. The rate constant for quinonoid intermediate formation from L-Trp is ∼10-fold lower for H463F Trpase than for wild-type Trpase, but the rate constant for reaction of L-Met is similar for H463F Trpase and wild-type Trpase. The temperature dependence of the rate constants for quinonoid intermediate formation reveals that both L-Trp and L-Met have similar values of $\Delta H^{\ddagger}$, but L-Met has a more negative value of $\Delta S^{\ddagger}$. Hydrostatic pressure perturbs the spectra of the H463F L-Trp and L-Met complexes, by shifting the position of the equilibria between different quinonoid and external aldimine complexes. Pressure-jump experiments show relaxations at 500 nm after rapid pressure changes of 100−400 bar with both L-Trp and L-Met. The apparent rate constants for relaxation of L-Trp, but not L-Met, show a significant increase with pressure. From these data, the value of $\Delta V^{\ddagger}$ for quinonoid intermediate formation from the external aldimine of L-Trp can be estimated to be −26.5 mL/mol, a larger than expected negative value for a proton transfer. These results suggest that there may be a contribution to the deprotonation reaction either from quantum mechanical tunneling or from a mechanical coupling of protein motion and proton transfer associated with the reaction of L-Trp, but not with L-Met.

Quinonoid intermediates play a critical role in the reactions catalyzed by pyridoxal 5′-phosphate-dependent enzymes. The quinonoid α-carbanionic intermediate is stabilized by resonance with the electron-withdrawing pyridinium ring of the PLP[1] cofactor, and exhibits an intense ($\epsilon \sim 4 \times 10^4$ M^{-1} cm^{-1}) visible absorption peak with a λ_{max} near 500 nm (*1*, *2*). These anionic intermediates can be formed in various reactions, by removal of the α-proton of the external aldimine of an amino acid by an active site base, by Michael addition of a nucleophile to an aminoacrylate, by α-decarboxylation, or by a retro-aldol reaction with cleavage of the $C_\alpha-C_\beta$ bond, as in the reaction of serine hydroxymethyltransferase. Tryptophan indole-lyase (Trpase, EC 4.1.99.1) is a PLP-dependent enzyme which catalyzes a reversible hydrolytic β-elimination reaction of L-Trp to form indole and ammonium pyruvate (eq 1).

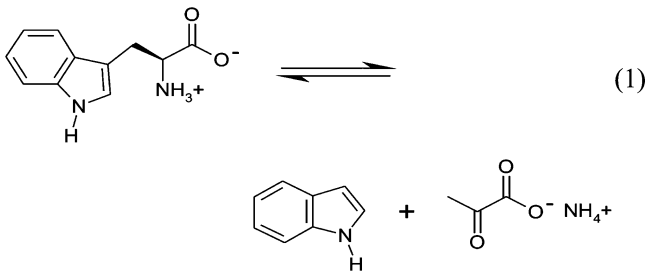

(1)

This enzyme is found in a wide variety of enteric bacteria, including *Escherichia coli* (*3*), *Proteus vulgaris* (*4*), *Hae-*

† This work was partially supported by a grant from the National Institutes of Health (GM-42588) to R.S.P.

* To whom correspondence should be addressed: Department of Chemistry, University of Georgia, Athens, GA 30602-2556. E-mail: rsphillips@chem.uga.edu. Phone: (706) 542-1996. Fax: (706) 542-9454.

‡ University of Georgia.

§ Max-Planck-Institut für Molekulare Physiologie.

[1] Abbreviations: PLP, pyridoxal 5′-phosphate; Trpase, tryptophan indole-lyase (tryptophanase) (EC 4.1.99.1); SOPC, *S*-(*o*-nitrophenyl)-L-cysteine; $E-Trp_{EA}$, external aldimine complex of H463F Trpase and L-Trp; $E-Trp_Q$, quinonoid complex of H463F Trpase and L-Trp.

10.1021/bi051062a CCC: $30.25
Published on Web 10/07/2005

Scheme 1

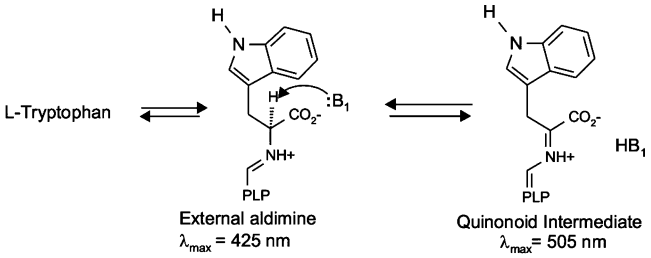

mophilus influenzae (*5*), and *Vibrio cholera* (*6*). It has been shown that the presence of the *tna*A gene, encoding Trpase, is necessary for virulence in *H. influenzae* (*5*). Recently, data have shown that Trpase plays an important role in regulation of biofilm formation in *E. coli* and other bacteria (*7*, *8*). In addition to the physiological reaction shown in eq 1, Trpase can also catalyze the β-elimination reactions in vitro of a wide range of amino acids with good leaving groups on the β-carbon, including *S*-(*o*-nitrophenyl)-L-cysteine (SOPC) (*9*), *S*-alkyl-L-cysteines (*10*), β-chloro-L-alanine (*10*), L-serine (*10*), and *O*-acyl-L-serines (*11*). Trpase from *E. coli* exhibits a spectrum in the steady state of the reaction with L-Trp consistent with a mixture of an external aldimine, absorbing at 425 nm, and a quinonoid intermediate, exhibiting an absorption peak at 505 nm, as shown in Scheme 1 (*12*−*17*). Trpase also forms equilibrating mixtures of quinonoid and external aldimine intermediates with a number of quasi-substrates without leaving groups on the β-carbon, and which do not undergo turnover, such as L-Ala and L-Met (*1*, *2*), but with considerably slower rate constants. H463F mutant Trpase was examined previously and found to have very low activity with L-Trp, but near wild-type activity with SOPC and *S*-ethyl-L-cysteine (*18*). His-463 was proposed to be involved in hydrogen bonding interactions with the indolic NH group of the L-Trp substrate which are critical for the β-elimination of indole, but which are less important for external aldimine and quinonoid intermediate formation (*18*, *19*). Hence, because of the low elimination activity, H463F Trpase forms a quasi-equilibrium mixture of external aldimine and quinonoid intermediates with L-Trp (Scheme 1) which resembles that of the steady state formed by wild-type Trpase (*18*). Thus, this mutant is useful in studying the mechanism of L-Trp binding and of quinonoid intermediate formation with Trpase. In this study, we have examined the effects of temperature and hydrostatic pressure on the equilibria and rate constants for quinonoid intermediate formation from L-Trp and L-Met with H463F Trpase.

EXPERIMENTAL PROCEDURES

Materials. S-(*o*-Nitrophenyl)-L-cysteine (SOPC) was prepared as previously described (*20*). Lactate dehydrogenase (LDH) from rabbit muscle, L-Tryptophan, *S*-ethyl-L-cysteine, PLP, L-methionine, and NADH were purchased from United States Biochemical Corp.

Enzyme Purification. The H463F mutant Trpase was purified by hydrophobic chromatography on a column of CL-Sepharose 4B, as described previously for wild-type Trpase (*21*), except that a gradient of $(NH_4)_2SO_4$ from 40 to 20% saturation was used for elution, rather than a stepwise elution. The amount of protein was determined in crude extracts by the method of Bradford (*22*), with purified wild-type Trpase as a standard. The concentration of purified wild-type and H463F mutant Trpase was determined from the absorbance at 278 nm ($A^{1\%} = 9.19$) (*21*). Enzyme activity during purification was routinely measured with 0.6 mM SOPC in 50 mM potassium phosphate at pH 8.0 and 25 °C (*9*), following the decrease in absorbance at 370 nm ($\Delta\epsilon = -1.86 \times 10^3\ M^{-1}\ cm^{-1}$) using a Cary 1E UV−vis spectrophotometer equipped with a 6 × 6 Peltier temperature-controlled cell compartment.

Stopped-Flow Reactions. Stopped-flow experiments were carried out using an RSM-1000 instrument from OLIS, Inc. (Bogart, GA), equipped with a stopped-flow mixing chamber, as described previously (*12*, *13*). The stopped-flow mixer has a 10 mm path length and a dead time of <2 ms. Absorbance spectra were collected over the wavelength range from 240 to 800 nm at a rate of 1000 scans/s. Enzymes for stopped-flow measurements were preincubated with excess PLP for 30 min, and then passed through a PD-10 gel filtration column equilibrated with 0.1 M triethanolamine hydrochloride (pH 8.0) and 0.1 M KCl, to remove excess PLP.

The concentration dependence experiments were performed with a final concentration of 1 mg/mL (18.3 μM active sites) H463F or wild-type Trpase, and varying concentrations of either L-Trp or L-Met, in 0.1 M triethanolamine hydrochloride (pH 8.0) and 0.1 M KCl at 20 °C. The L-Trp concentrations were 0.5, 1.0, 2.0, 4.0, 8.0, 16.0, and 20.0 mM. The L-Met concentrations were 4, 8, 16, 32, 64, and 100 mM. The temperature of the reactions was controlled by circulating water from a Lauda water bath through the stopped-flow apparatus. Temperatures were measured in the stopped-flow mixer with a thermometer and did not vary more than 0.5 °C during the collection of the data. The temperature dependence experiments were performed with 1 mg/mL (18.3 μM active sites) H463F Trpase and either 16 mM L-Trp or 100 mM L-Met, in 0.1 M triethanolamine hydrochloride (pH 8.0) and 0.1 M KCl.

Absorption Spectra under Hydrostatic Pressure. The effects of hydrostatic pressure on the absorption spectra were measured using a Cary 14 UV−vis spectrophotometer modified by OLIS, Inc., to contain a high-pressure cell from ISS (Champaign, IL), equipped with a manual pressure pump. The cell was maintained at 25 °C with an external circulating water bath. The enzyme solutions were contained in 1 mL quartz bottles with a 9 mm path length, capped with Teflon tubing and immersed in spectroscopic-grade ethanol as the pressurizing fluid. A buffer blank at 1 bar was used to obtain a baseline reading. The buffer, triethanolamine hydrochloride (pH 8.0), was chosen since the pK_a is 7.88 and the ΔV_o for ionization is 4.5 ± 0.3 mL/mol (*23*); therefore, the pressure change will not significantly change the pH. The enzyme solutions were scanned at 1 bar, and immediately after the increase in pressure to 400 bar. The difference spectra were calculated by subtraction of the 1 bar spectra from the 400 bar spectra.

Pressure-Jump Experiments. These experiments were carried out in a home-built pressure-jump (p-jump) instrument described previously (*24*, *25*). The pressure perturbations that were applied ranged from 100 to 400 bar in 50 bar steps. A pre-pressure of approximately 10 bar was applied to the sample. The pressure change was monitored by a transducer; the pressure increase was 90% complete within

100 μs, and the decrease was 90% complete within 50 μs. Typically, 20−100 transients were collected and averaged, with collection of 1000 data points for 1 s following the pressure increase, a short delay (1−2 s) between the end of data collection and the pressure release, and collection of 1000 data points for 1 s following the pressure decrease. The temperature of the sample was measured by a Pt 100 sensor in contact with the cell and controlled by a circulating water bath at 25.0 °C.

Data Analysis. The rapid-scanning stopped-flow data were analyzed by global analysis of all spectra at all wavelengths using the Globalworks program provided by OLIS (*26*). The spectra were fitted to the minimum number of species and exponential processes to adequately describe the data based on residuals and standard deviation, using eq 2, where A_t is the absorbance at a wavelength at time t, A_i is the absorbance at that wavelength for each phase, k_i is the rate constant for each phase, and A_∞ is the final absorbance at that wavelength of the reaction mixture. The pressure-jump single-wavelength data were also analyzed by fitting to eq 2 using the software obtained from OLIS, Inc. The rate constants obtained at various L-Trp or L-Met concentrations were fit to eq 3 (*27*), where k_f is the rate constant in the forward direction, k_r is the rate constant for the reverse reaction, and K_d is the apparent binding constant for ligand, L.

$$A_t = \sum A_i \exp(-k_i t) + A_\infty \quad (2)$$

$$k_{obs} = (k_f[L])/(K_d + [L]) + k_r \quad (3)$$

Effects of Temperature and Pressure. The effect of temperature on a rate constant is given by eq 4, the Eyring equation, where k_B is the Boltzman constant and h is Planck's constant. In logarithmic form, eq 4 gives eq 5, which can be rearranged to eq 6. Thus, the slope of a plot of ln k − ln k_BT/h against $1/T$ is $\Delta H^{\ddagger}/R$, and the intercept is $\Delta S^{\ddagger}/R$. The effect of pressure on rate constants is given by eq 7, which is analogous to the Eyring equation, where k_P is the rate constant at pressure P, k_0 is the rate constant at 1 bar, and $\Delta V^{\ddagger}$ is the activation volume.

$$k = (k_BT/h)\exp(-\Delta G^{\ddagger}/RT) = (k_BT/h)\exp(-\Delta H^{\ddagger}/RT + \Delta S^{\ddagger}/R) \quad (4)$$

$$\ln k = \ln(k_BT/h) - \Delta H^{\ddagger}/RT + \Delta S^{\ddagger}/R \quad (5)$$

$$\ln k - \ln(k_BT/h) = \Delta S^{\ddagger}/R - \Delta H^{\ddagger}/RT \quad (6)$$

$$k_P = k_o \exp(-P\Delta V^{\ddagger}/RT) \quad (7)$$

RESULTS

Rapid-Scanning Stopped-Flow Reaction of H463F Trpase with L-Trp and L-Met. The reaction of H463F Trpase with L-Trp was followed by rapid-scanning stopped-flow spectrophotometry (Figure 1). In the first phase of the reaction, there is a rapid increase in absorbance to form a quinonoid intermediate, with λ_{max} at 501 nm, and a corresponding decrease in absorbance of the external aldimine at 414 nm (Figure 1A). In the second phase, there is an additional increase in the intensity of the absorbance at 501 nm. The two phases are clearly seen in the spectra (Figure 1A) and time courses at 501 and 414 nm (Figure 1B). The reaction of H463F Trpase with L-Met also exhibits the formation of external aldimine and quinonoid intermediates (Figure 2A). As with L-Trp, the reaction requires two exponentials to obtain a good fit of the data. The first phase shows a decrease in absorbance at 415 nm for the external aldimine and an increase in the absorbance of the quinonoid band at 501 nm, while the second phase is associated with an increase in the 501 nm absorbance (Figure 2B).

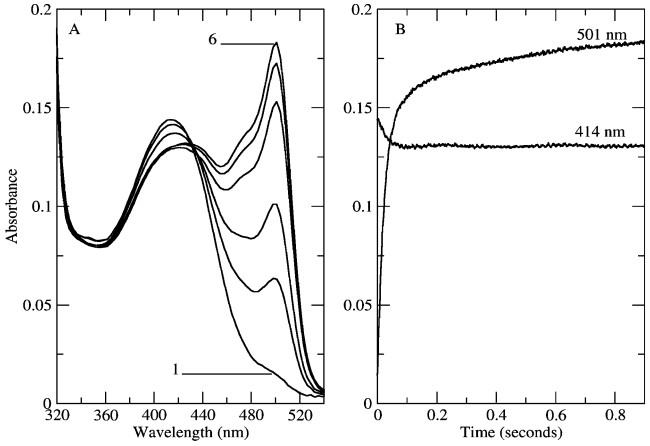

FIGURE 1: Rapid-scanning stopped-flow spectra of the reaction of H463F Trpase with L-Trp. The reaction mixture contained 18.3 μM H463F Trpase and 20 mM L-Trp in 0.1 M triethanolamine hydrochloride (pH 8.0) and 0.1 M KCl. (A) The scans are shown (1) 0.002, (2) 0.010, (3) 0.023, (4) 0.090, (5) 0.360, and (6) 0.900 s after mixing. (B) Time courses for the reaction at 414 and 505 nm.

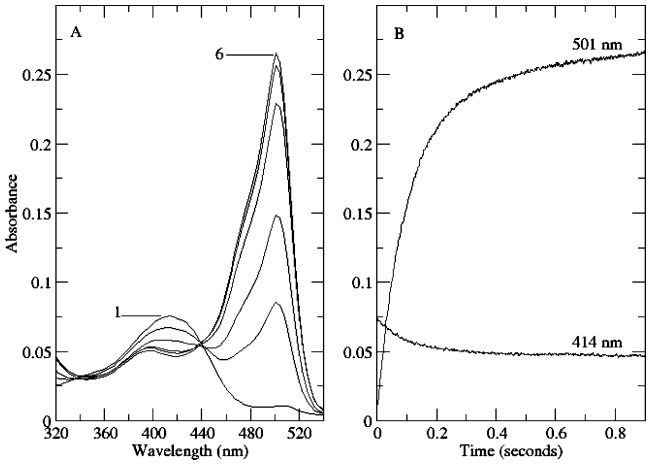

FIGURE 2: Rapid-scanning stopped-flow spectra of the reaction of H463F Trpase with L-Met. The reaction mixture contained 18.3 μM H463F Trpase and 100 mM L-Met in 0.1 M triethanolamine hydrochloride (pH 8.0) and 0.1 M KCl. (A) The scans are shown (1) 0.002, (2) 0.041, (3) 0.092, (4) 0.273, (5) 0.580, and (6) 0.900 s after mixing. (B) Time courses for the reaction at 414 and 501 nm.

The apparent rate constant for the fast phases of the reactions exhibits a hyperbolic dependence on L-Trp and L-Met concentration (Figure 3), while the rate constants of the slow phases are independent of ligand concentration (data not shown). Fitting of the concentration dependence of the fast phase of the data with H463F Trpase to eq 3 gives an apparent K_d of 3.04 ± 0.57 mM, a k_f of 37.4 ± 1.3 s^{-1}, and a k_r of 17.0 ± 1.6 s^{-1} for L-Trp and a K_d of 40.5 ± 12.8 mM, a k_f of 14.3 ± 1.2 s^{-1}, and a k_r of 1.1 ± 0.6 s^{-1} for L-Met, at 20 °C. The slow phases with both L-Trp and L-Met

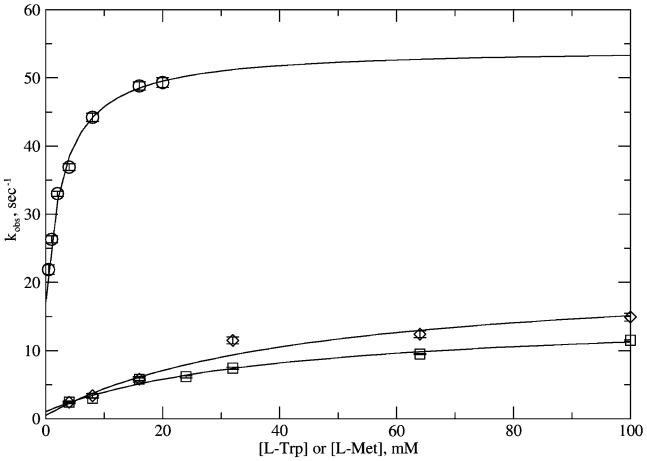

FIGURE 3: Concentration dependence of the fast rate constant for quinonoid intermediate formation from L-Trp and L-Met: (○) H463F with L-Trp, (□) H463F with L-Met, and (◇) wild type with L-Met. The lines are the fitted curves to eq 3.

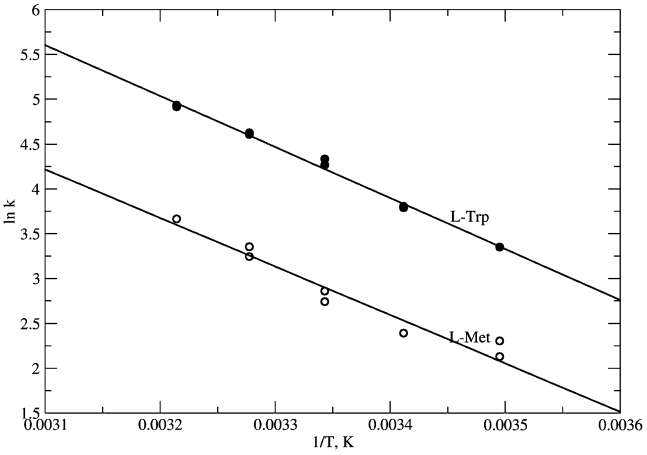

FIGURE 4: Temperature dependence of the apparent rate constants for quinonoid intermediate formation from L-Trp and L-Met. The rate constants were measured at 16 mM L-Trp and 100 mM L-Met: (●) L-Trp and (○) L-Met. The lines are the result of regression analysis of the data.

exhibit similar rate constants, ~2−3 s^{-1}. The rate constant for quinonoid intermediate formation from L-Trp by H463F Trpase is ~10-fold lower than that of wild-type Trpase (*1*, *2*, *12*, *13*, *17*), while the rate constant for quinonoid intermediate formation of L-Met by H463F Trpase is very similar that of wild-type Trpase (Figure 3), which has a K_d of 43.8 ± 21.6 mM, a k_f of 21.0 ± 3.9 s^{-1}, and a k_r of 0.46 ± 0.98 s^{-1}. The temperature dependence of the apparent rate constants for quinonoid intermediate formation for H463F Trpase at 16 mM L-Trp and 100 mM L-Met is shown in Figure 4. From these plots, the values of $\Delta H^{\ddagger}$ and $\Delta S^{\ddagger}$ for quinonoid intermediate formation from L-Trp and L-Met for H463F Trpase can be obtained with eq 6. The values of $\Delta H^{\ddagger}$ are 47.3 ± 1.6 kJ/mol for L-Trp and 45.0 ± 3.5 kJ/mol for L-Met; the values of $\Delta S^{\ddagger}$ are −51.0 ± 1.4 J mol^{-1} K^{-1} ($-T\Delta S^{\ddagger}$ = 15.2 kJ/mol at 298 K) for L-Trp and −69.7 ± 4.6 J mol^{-1} K^{-1} ($-T\Delta S^{\ddagger}$ = 20.8 kJ/mol at 298 K) for L-Met.

Effects of Pressure on Spectra of H463F Trpase with L-Trp and L-Met. When solutions of H463F Trpase complexed with L-Trp or L-Met are subjected to increased hydrostatic pressure, changes in the absorption spectra of the PLP−amino acid complexes are observed. The difference spectra between solutions at 400 and 1 bar are shown in Figure 5.

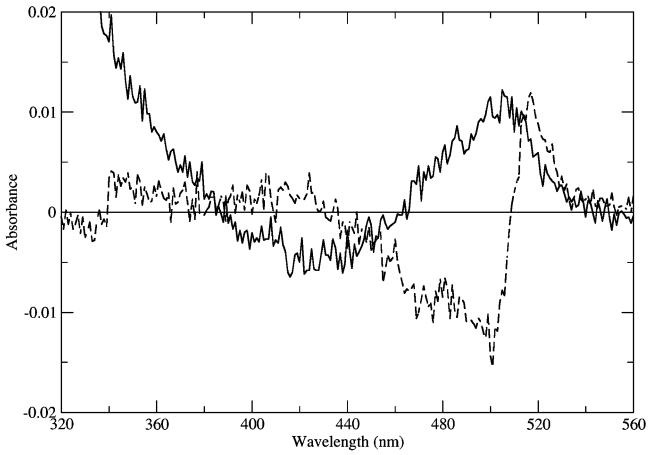

FIGURE 5: Difference spectra of the H463F Trpase complex with L-Trp and L-Met. The solutions contained 29 μM H463F Trpase and 20 mM L-Trp or 100 mM L-Met in 0.1 M triethanolamine hydrochloride (pH 8.0) and 0.1 M KCl: (solid line) difference spectrum between 400 and 1 bar for L-Trp and (dashed line) difference spectrum between 400 and 1 bar for L-Met.

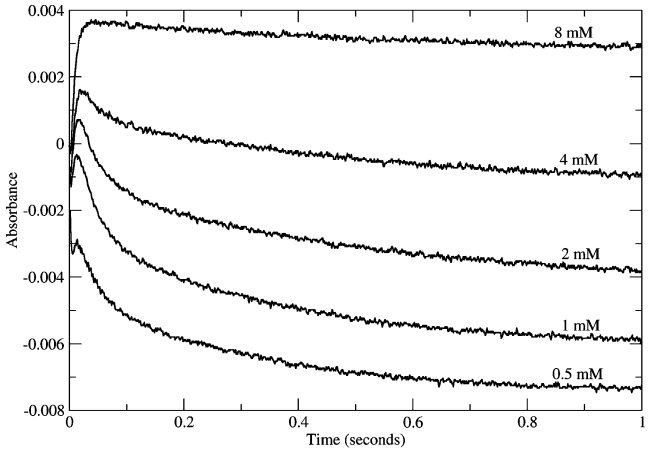

FIGURE 6: Relaxations after a pressure jump for the complex of H463F Trpase with various concentrations of L-Trp. The reaction mixtures contained 74.4 μM H463F Trpase and the indicated L-Trp concentration in 0.1 M triethanolamine hydrochloride (pH 8.0) and 0.1 M KCl. The pressure change was 400 bar.

The complex of H463F Trpase with L-Trp shows an increase in the magnitude of the quinonoid absorption band at ~505 nm, and a corresponding decrease in the absorbance at 430 nm for the external aldimine, when the pressure is increased to 400 bar (Figure 5, solid line). The difference spectra for the complex of H463F Trpase with L-Met show a slight red shift in the absorption maximum from 505 to 508 nm when the pressure is increased to 400 bar, without any significant change in the spectrum from 300 to 460 nm (Figure 5, dashed line). The red shift of the absorption maximum is evident from the derivative shape of the difference spectrum with L-Met.

Pressure Jump of H463F Trpase with L-Trp and L-Met. When the solutions of H463F Trpase with L-Trp and L-Met were subjected to rapid pressure changes of 100−400 bar in a pressure-jump instrument, relaxations at 500 nm are observed (Figure 6). The time courses of the relaxations change with L-Trp concentration. At low L-Trp concentrations, there is a rapid relaxation of low amplitude with increasing absorbance, followed by a biphasic decay with a larger amplitude, with k_{obs} values of ~30 s^{-1} ($1/\tau_2$) and 3

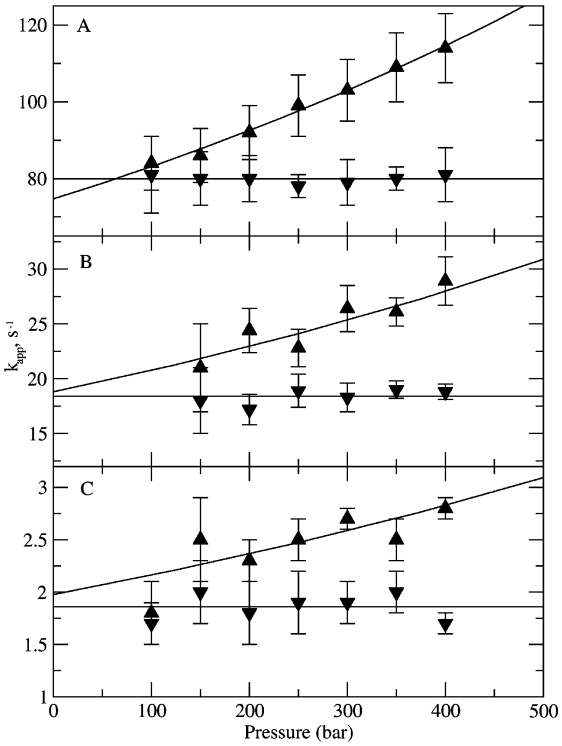

FIGURE 7: Dependence of k_{app} for the relaxation with pressure for L-Trp: (▲) relaxation after the push to high pressure and (▼) relaxation after the release to 10 bar. The error bars show the standard errors obtained from curve fitting. (A) Rate constants for relaxation of the fast phase ($1/\tau_1$) of increasing absorbance for data collected with 20 mM L-Trp. The curve through the upward-pointing triangles is the calculated curve for the fit to eq 7. The line through the downward-pointing triangles is the average of the values. (B) Rate constants for relaxation of the intermediate phase ($1/\tau_2$) of decreasing absorbance for data collected at 1 mM L-Trp. The curve through the upward-pointing triangles is the calculated curve for the fit to eq 7. The line through the downward-pointing triangles is the average of the values. (C) Rate constants for relaxation of the slow phase ($1/\tau_3$) of decreasing absorbance for data collected at 1 mM L-Trp. The curve through the upward-pointing triangles is the calculated curve for the fit to eq 7. The line through the downward-pointing triangles is the average of the values.

s^{-1} ($1/\tau_3$) (Figure 6). However, at >8 mM L-Trp, there is a rapid relaxation with a relatively large increase in absorbance ($1/\tau_1$), followed by a single-exponential decay of low amplitude, with a k_{obs} of ~3 s^{-1}. The rate constant of the fast relaxation, $1/\tau_1$, increases with an increase in pressure (Figure 7A, upward-pointing triangles), ranging from 84 to 114 s^{-1} over the pressure range from 100 to 400 bar. The corresponding apparent rate constant for the formation of the quinonoid species from stopped-flow experiments at 25 °C is 71 s^{-1}, in good agreement with the intercept value of 75 s^{-1} in Figure 7. The average value of the rate constant measured after the release of pressure back to 10 bar is 79.9 s^{-1} (Figure 7A, downward-pointing triangles). From fitting of the data in Figure 7A to eq 7, $\Delta V^{\ddagger}$ can be determined to be -26.5 ± 1.2 mL/mol. The intermediate relaxation, $1/\tau_2$ (Figure 7B), and the slow relaxation, $1/\tau_3$ (Figure 7C), processes also show significant increases in rate constant with pressure, with $\Delta V^{\ddagger}$ values of -24.6 ± 6.2 and -22.3 ± 9.2 mL/mol, respectively.

When solutions of H463F and wild-type Trpase with L-Met are exposed to a rapid pressure change of 100−400 bar in the pressure-jump instrument, relaxations at 500 nm are also observed (Figure 8), which are biphasic. As expected from

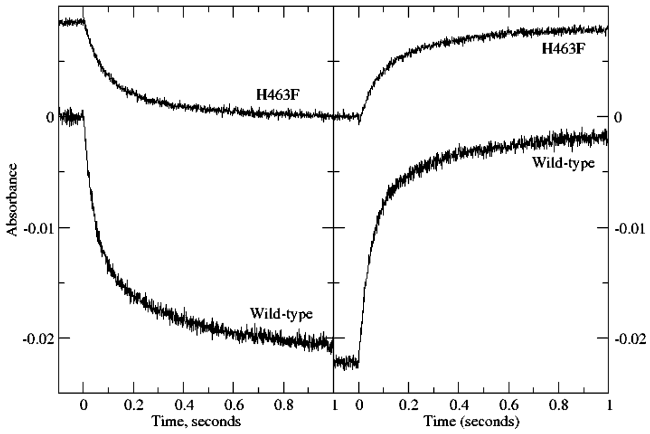

FIGURE 8: Relaxations after the pressure jump for the complex of wild-type and H463F Trpase with L-Met. The reaction mixtures contained 74.4 μM wild-type or H463F Trpase and 100 mM L-Met in 0.1 M triethanolamine hydrochloride (pH 8.0) and 0.1 M KCl. The pressure change was 400 bar. At the left is the relaxation after the pressure increase. At the right is the relaxation after the pressure release to 10 bar.

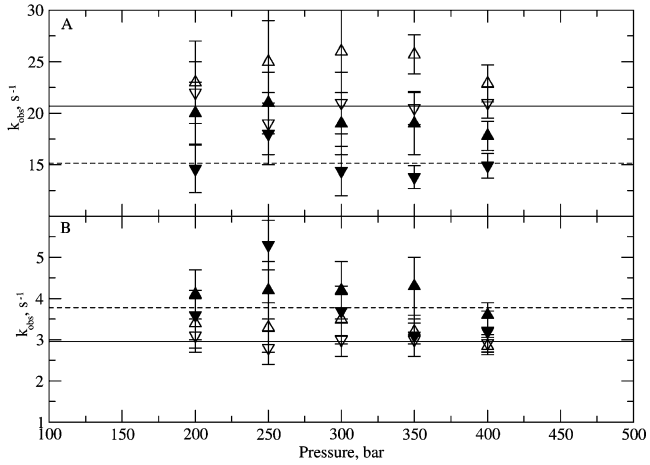

FIGURE 9: Dependence of k_{app} for the relaxation with pressure for L-Met: (upward-pointing triangles) relaxation after the push to the indicated pressure and (downward-pointing triangles) relaxation after the release from the indicated pressure to 10 bar. The error bars show the standard errors obtained from curve fitting. (A) Rate constants for relaxation of the fast phase ($1/\tau_1$) of decreasing absorbance for data collected with 100 mM L-Met. The solid line through the empty downward-pointing triangles is the average of the values for wild-type Trpase, and the dashed line through the filled downward-pointing triangles is the average of the values for H463F Trpase. (B) Rate constants for relaxation of the slow phase ($1/\tau_2$) of decreasing absorbance for data collected at 100 mM L-Met. The solid line through the empty downward-pointing triangles is the average of the values for wild-type Trpase, and the dashed line through the filled downward-pointing triangles is the average of the values for H463F Trpase.

the difference spectra shown in Figure 6, the absorbance at 500 nm decreases in the relaxations. In contrast to the data obtained with H463F Trpase and L-Trp, with L-Met and either wild-type or H463F mutant Trpase, there is no significant change in the observed rate constants with pressure over the range from 100 to 400 bar (Figure 9).

DISCUSSION

H463F Trpase is a mutant enzyme which catalyzes rapid β-elimination reactions with nonphysiological substrates such as *S*-ethyl-L-Cys and SOPC, but has a very slow rate of

turnover (<0.1% of the wild-type rate) with L-Trp (*18*). However, H463F Trpase forms a quasi-equilibrium complex with L-Trp which exhibits a visible spectrum that closely resembles that seen in the steady state of the reaction of wild-type Trpase (Figure 1). Thus, the effect of the H463F mutation on activity is primarily on the step of elimination of indole in the reaction of L-Trp, and hence, the H463F mutant Trpase is a useful model for studying the mechanism of L-Trp binding and quinonoid intermediate formation by Trpase.

The calculated rate constant for formation of the quinonoid intermediate of L-Trp is 71 s^{-1} at 25 °C, compared to 760−900 s^{-1} for wild-type Trpase at 25 °C (*12*−*17*). Thus, there is an ∼10-fold reduction in the rate constant for quinonoid intermediate formation resulting from the mutation. In contrast, the rate constant for quinonoid intermediate formation from L-Met by H463F Trpase is very similar to that with L-Met and wild-type Trpase (Figure 2) and with that reported for the reaction of the wild-type enzyme and L-ethionine (*1*). These results are consistent with earlier studies that found the indole NH group on the substrate side chain is important for rapid quinonoid intermediate formation by wild-type Trpase (*17*), most likely because of hydrogen bonding of the side chain indole NH group with a catalytic base with a pK_a of ∼6 previously seen in the pH dependence of k_{cat}/K_m for L-Trp (*28*). Since His-463 may be the proposed catalytic base, or be associated with it (*18*, *19*), the elimination of the hydrogen bond between the indole ring and the protein, by removal of either the substrate NH donor or the protein acceptor, would be expected to have a similar effect on the rate constant for quinonoid intermediate formation. The temperature dependence of the rate constant for quinonoid intermediate formation shows a similar value of $\Delta H^{\ddagger}$ for both L-Trp and L-Met (Figure 4), but a significantly larger negative value of $\Delta S^{\ddagger}$ for L-Met. The main reason for the approximate 3-fold difference in the rate constants for quinonoid intermediate formation of L-Trp and L-Met is thus entropic in origin. This suggests that there is a larger amount of active site reorganization required to reach the transition state for quinonoid intermediate formation in the reaction of L-Met than that of L-Trp.

When the complexes of H463F Trpase with L-Trp and L-Met are subjected to increased hydrostatic pressure, there are distinct changes in the absorption spectra, which are more easily seen in the difference spectra (Figure 5). For the L-Trp complex, the difference spectrum between 400 and 1 bar exhibits an increase in absorbance of the 505 nm band, and a decrease in absorbance centered around 425 nm, indicating that pressure affects the internal equilibrium between the external aldimine and quinonoid intermediates in the direction of the quinonoid species (Figure 5, solid line). Thus, the quinonoid form of the enzyme has a smaller net volume than the external aldimine. As expected from the data in Figure 5, when the equilibrium mixtures of H463F Trpase and L-Trp are subjected to rapid pressure changes of 100−400 bar in the pressure-jump instrument, relaxations result. The time courses of the relaxations with L-Trp are strongly concentration dependent (Figure 6). At higher L-Trp concentrations, ≥8 mM, where the binding equilibrium is nearly saturated, there is a large amplitude fast relaxation, $1/\tau_1$, of increasing absorbance, which exhibits a rate constant comparable to that seen for quinonoid intermediate formation in the stopped-flow experiments. Thus, this relaxation corresponds to the interconversion of external aldimine and quinonoid intermediates ($k_1 + k_{-1}$), and it exhibits a significant pressure dependence, with the rate increasing with pressure, as can be seen in Figure 7A, with an apparent $\Delta V^{\ddagger}$ of −26.5 mL/mol.

At 0.5 and 1 mM L-Trp, well below the K_d of 3 mM for L-Trp, the fast relaxation is observed; however, it is very small in amplitude, and it is followed by a slower absorbance decrease, with a much larger amplitude, which is biphasic (Figure 6). The decrease in absorbance at 500 nm in the intermediate phase, $1/\tau_2$, at low L-Trp concentrations implies that pressure negatively affects the L-Trp binding equilibrium, resulting in a decreased level of binding at high pressure, and the quinonoid intermediate will thus decay to reach the new equilibrium. The effect of pressure on the binding equilibrium is likely the result of solvation differences between the free enzyme and L-Trp complex. If L-Trp binding results in the release of bound active site water, as well as water associated with solvation of the amino acid in solution, to the bulk solvent, there will be a net increase in system volume, which will be opposed by pressure. The simplest model which can explain the stopped-flow results as well as the fast and intermediate relaxations observed in the pressure jump with L-Trp is shown in eq 8. The corresponding rate equations for the relaxations at high and low L-Trp concentrations are given by eqs 9 and 10, respectively. There is good agreement of the rate constant for the intermediate relaxation from Figure 7B (18 s^{-1}) with the intercept value in Figure 3 (17 s^{-1}), which is the rate constant for reprotonation of the quinonoid species. Since this relaxation is dominated by the reprotonation term, k_{-1}, when [L-Trp] < K_d in eq 10, this is expected. The rate constant for this process also exhibits a significant dependence on pressure, increasing as the pressure is increased (Figure 7B). Fitting the data for $1/\tau_2$ to eq 7 gives an apparent $\Delta V^{\ddagger}$ of −24.6 mL/mol, very similar to that of the fast phase. If the equilibrium constant for a process is close to 1, the activation volume will be the same in both directions. On the basis of the stopped-flow data shown in Figure 3, the equilibrium constant for the external aldimine−quinonoid interconversion is 2.2.

$$\text{E} + \text{L-Trp} \overset{K_d}{\rightleftharpoons} \text{E}-\text{Trp}_{EA} \overset{k_1}{\underset{k_{-1}}{\rightleftharpoons}} \text{E}-\text{Trp}_{EQ} \qquad (8)$$

$$k_{obs} = 1/\tau_1 = k_1 + k_{-1} \qquad (9)$$

$$k_{obs} = 1/\tau_1 = k_1[\text{Trp}]/(K_d + [\text{Trp}]) + k_{-1} \qquad (10)$$

The slowest phase of the relaxation with L-Trp, $1/\tau_3$, also exhibits a dependence of rate constant on pressure (Figure 7C). This relaxation also corresponds to the slow phase observed in the stopped-flow experiments. This slow process exhibits an activation volume similar to those of other phases, with an apparent $\Delta V^{\ddagger}$ of −22.3 mL/mol. The similar pressure dependence of the slow rate constant to the fast and intermediate phases suggests that this step involves a deprotonation reaction, rather than an isomerization of the preformed quinonoid intermediate. Thus, the slowest relaxation appears to be coming from a second quinonoid complex which forms from an external aldimine. Previous stopped-flow studies of wild-type Trpase with L-methionine found

biphasic kinetics for quinonoid intermediate formation, and the authors concluded that there are two different enzyme forms with different reactivities that are slowly interconverted (*1*). A similar result was seen in the reaction of tyrosine phenol-lyase, where biphasic kinetics of quinonoid intermediate formation from L-tyrosine were proposed to be due to high- and low-activity forms of the enzyme (*29*). The interconversion of the high- and low-activity forms of tyrosine phenol-lyase is much slower, at a rate of $\sim$0.3 s^{-1}, than formation of the external aldimine and quinonoid complex (*29*). The equilibrium between high- and low-activity forms of Trpase and TPL is affected by monovalent cations, particularly K^+ and NH_4^+ (*1*, *29*−*31*).

In contrast, the difference spectra for the H463F Trpase−L-Met complex between 1 and 400 bar show a change in the absorbance of the quinonoid intermediate, due to a 3 nm red shift of λ_{max}, and no change in absorbance in the 425 nm region (Figure 5, dashed line). This result suggests that hydrostatic pressure primarily affects the equilibrium between different quinonoid complexes of L-Met, rather than between the external aldimine and quinonoid intermediates. In this case, the two quinonoid species must have different absorption maxima and different reaction volumes. When the L-Met complex of either H463F or wild-type Trpase is subjected to pressure jumps of 100−400 bar, relaxations are observed, which are also biphasic (Figure 8). The biphasic reaction is likely due to the high- and low-activity forms of the enzyme, as discussed above. There is good agreement about the rate constants for the fast phase of the reaction of H463F Trpase with 100 mM L-Met obtained by stopped-flow (12 s^{-1}) and pressure-jump (15 s^{-1}) methods. In contrast to the data with L-Trp, neither of the apparent rate constants for the relaxations with L-Met shows any significant pressure dependence for either wild-type or H463F Trpase (Figure 9). This suggests that $\Delta V^{\ddagger}$ is significantly reduced for the reaction of L-Met, likely approximately −10 mL/mol or less.

The formation of the quinonoid intermediates of L-Trp and L-Met with Trpase involves the abstraction of a proton by a base from the α-C−H bond of the amino acid, bound as a Schiff base to the PLP. The $\Delta V^{\ddagger}$ for formation of the quinonoid complex of L-Trp with H463F Trpase is −26.5 mL/mol. In contrast, the $\Delta V^{\ddagger}$ for a proton transfer is normally expected to lie in the range from −5 to −15 mL/mol (*32*), in the absence of solvation of the resultant ion pair, which results in electrostriction. It is highly unlikely that the chemically reactive quinonoid intermediates formed in PLP-dependent enzyme reactions are solvent-exposed, so a contribution to the $\Delta V^{\ddagger}$ due to electrostriction can be ruled out. What, then, is the physical basis of the large negative $\Delta V^{\ddagger}$ observed for the reaction of H463F Trpase with L-Trp? Isaacs reviewed the effects of pressure on isotope effects for a number of chemical reactions which involve hydrogen transfer (proton, hydrogen atom, and hydride), and several of them which are suspected of exhibiting quantum mechanical hydrogen tunneling exhibit anomalously large negative $\Delta V^{\ddagger}$ values. For example, the base-catalyzed iodination reaction of 2-nitropropane, which exhibits rate-determining proton abstraction, shows a large primary kinetic deuterium isotope effect, k_H/k_D, of 16−20; $\Delta V^{\ddagger}$ is −31 mL/mol for the protio substrate and −40 mL/mol for the deuterio substrate (*32*). Thus, it is possible that the large negative $\Delta V^{\ddagger}$ that we observe for the reaction of L-Trp is due to a contribution of tunneling to the proton transfer reaction. While the formation of the quinonoid intermediate of L-Trp by wild-type Trpase exhibits a deuterium isotope effect of 3.6 (*15*), primary deuterium isotope effects greater than the semiclassical limit of 7−8 are not always a requirement for tunneling. Quantum mechanical tunneling has been shown to contribute to catalysis in a number of enzymatic reactions which involve hydrogen transfer, including proton transfer in bovine serum amine oxidase (*33*), hydride transfer in horse liver alcohol dehydrogenase (*34*) and dihydrofolate reductase (*35*), and hydrogen atom transfer in soybean lipoxygenase (*36*). However, despite that fact that many PLP-dependent enzymes normally deprotonate C−H bonds in their reactions, there have been few previous reports of hydrogen tunneling in these reactions. Cook et al. (*37*) proposed that an increase in the primary kinetic isotope effect observed in the β-elimination reaction of *O*-acetylserine sulfhydrylase substituted with a cofactor analogue may be due to an increase in the extent of hydrogen tunneling.

While it is generally agreed that large negative activation volumes and decreasing kinetic isotope effects with increasing pressure for hydrogen transfers are characteristic of quantum mechanical tunneling in chemical reactions (*38*, *39*), there have been only a few reports of these phenomena in enzymatic reactions. Northrop and Cho (*40*) and Park et al. (*41*) measured the effects of hydrostatic pressure on the deuterium isotope effect in the reaction of yeast alcohol dehydrogenase with benzyl alcohol and 2-propanol, and they observed large negative $\Delta V^{\ddagger}$ values of -39.9 ± 1.0 and -29.6 ± 2.0, respectively, for the hydride transfer. The $\Delta V^{\ddagger}$ values were found to be even more negative for the deuterated substrates of yeast alcohol dehydrogenase, so the kinetic isotope effects decrease at high pressures. They concluded that the primary deuterium isotope effect in that reaction is due solely to a transition state phenomenon, without any significant semiclassical contribution from zero-point energy differences. Northrop and Cho (*40*) and Park et al. (*41*) suggested that the isotope effect in yeast alcohol dehydrogenase may arise from a mechanical mechanism which couples protein motion to the hydrogen transfer. This may be an alternative explanation for our results with L-Trp. In contrast, Quirk and Northrop found that formate dehydrogenase exhibits a relatively small negative $\Delta V^{\ddagger}$ of -9.7 ± 1.0 mL/mol, and it exhibits an increase in the kinetic isotope effect at high pressures (*42*).

Why is there such a difference in the magnitude of $\Delta V^{\ddagger}$ for the quinonoid intermediate formation of L-Trp and L-Met external aldimines by H463F Trpase, even though both reactions exhibit similar values of $\Delta H^{\ddagger}$? Both amino acids form equilibrating mixtures of external aldimine and quinonoid intermediates with the enzyme; however, the equilibrium position lies much farther in the direction of the quinonoid form for the L-Met complex. The L-Met quinonoid complex is also a dead end, since there is no suitable β-leaving group for elimination to proceed. The side chain of L-Met can provide relatively little binding energy, besides van der Waals interactions, that can assist in the deprotonation reaction. The indole ring in the side chain of the L-Trp substrate must make additional contacts with the enzyme, due to electrostatics, hydrogen bonding, and π-stacking, that can be used to preorganize the active site base and the external aldimine in the ground state, as shown by the lower activation entropy.

Furthermore, the interactions of the L-Trp side chain with the active site clearly must contribute to the reaction to increase the $\Delta V^{\ddagger}$, either by changing the width of the energy barrier to facilitate quantum mechanical tunneling or by enhancing the mechanical coupling of protein motion with proton transfer. If this interpretation is correct, it predicts that the kinetic isotope effect for quinonoid intermediate formation from L-Trp, but not L-Met, should show a decrease with an increase in pressure. These experiments are now in progress.

CONCLUSIONS

Since Trpase forms external aldimine and quinonoid complexes with substrates as well as with quasi-substrates such as L-Ala and L-Met, it has often been assumed that these quasi-substrates react in the same way as substrates, except that they do not contain a β-substituent that is a leaving group, and are thus suitable models for studying the mechanism of substrate binding and quinonoid intermediate formation. In this study, we have found that L-Trp and L-Met exhibit a number of subtle but significant differences in their interactions with H463F Trpase. First, there is a 3-fold difference in the rate constant for quinonoid intermediate formation. Although $\Delta H^{\ddagger}$ values are similar for both L-Trp and L-Met, $\Delta S^{\ddagger}$ is significantly more negative for L-Met, suggesting that the reaction of L-Trp requires less organization to reach the transition state. The effects of pressure on the spectra of the equilibrium mixtures are different as well, with the L-Met quinonoid complex showing a 3 nm red shift in the quinonoid absorption peak under pressure, while the L-Trp complex increases in intensity at 500 nm, without a red shift. Finally, the pressure dependence of the rate constants for quinonoid intermediate formation is much stronger for L-Trp than L-Met, with a negative activation volume, suggesting that there may be hydrogen tunneling or motion of the protein coupled with the quinonoid intermediate formation of L-Trp, but not for the reaction of L-Met.

ACKNOWLEDGMENT

The high-pressure cell from ISS, Inc., was purchased with a grant from the University of Georgia Research Foundation. We thank Dr. Roger S. Goody for helpful suggestions and comments on the manuscript.

REFERENCES

1. June, D. S., Suelter, C. H., and Dye, J. L. (1981) Equilibrium and Kinetic Study of Interaction of Amino Acid Inhibitors with Tryptophanase: Mechanism of Quinonoid Intermediate Formation, *Biochemistry 20*, 2714−2719.
2. Metzler, C. M., Viswanath, R., and Metzler, D. E. (1991) Equilibria and Absorption Spectra of Tryptophanase, *J. Biol. Chem. 266*, 9374−9381.
3. Morino, Y., and Snell, E. E. (1967) The Relation of Spectral Changes and Tritium Exchange Reactions to the Mechanism of Tryptophanase-catalyzed Reactions, *J. Biol. Chem. 242*, 2800−2809.
4. Kamath, A. V., and Yanofsky, C. (1992) Characterization of the Tryptophanase Operon of *Proteus vulgaris*. Cloning, Nucleotide Sequence, Amino Acid Homology, and in vitro Synthesis of the Leader Peptide and Regulatory Analysis, *J. Biol. Chem. 267*, 19978−19985.
5. Martin, K., Morlin, G., Smith, A., Nordyke, A., Eisenstark, A., and Golomb, M. (1998) The Tryptophanase Gene Cluster of *Haemophilus influenzae* Type b: Evidence for Horizontal Gene Transfer, *J. Bacteriol. 180*, 107−118.
6. Heidelberg, J. F., Eisen, J. A., Nelson, W. C., Clayton, R. A., Gwinn, M. L., Dodson, R. J., Haft, D. H., Hickey, E. K., Peterson, J. D., Umayam, L., Gill, S. R., Nelson, K. E., Read, T. D., Tettelin, H., Richardson, D., Ermolaeva, M. D., Vamathevan, J., Bass, S., Qin, H., Dragoi, I., Sellers, P., McDonald, L., Utterback, T., Fleishmann, R. D., Nierman, W. C., and White, O. (2000) DNA Sequence of both Chromosomes of the Cholera Pathogen *Vibrio cholerae*, *Nature 406*, 477−483.
7. Di Martino, P., Merieau, A., Phillips, R., Orange, N., and Hulen, C. (2002) Isolation of an *Escherichia coli* Strain Mutant Unable to form Biofilm on Polystyrene and to Adhere to Human Pneumocyte Cells: Involvement of Tryptophanase, *Can. J. Microbiol. 48*, 132−137.
8. Di Martino, P., Fursy, R., Bret, L., Sundararaju, B., and Phillips, R. S. (2003) Indole can act as an Extracellular Signal to Regulate Biofilm Formation in *Escherichia coli* and in Other Indole-producing Bacteria, *Can. J. Microbiol. 49*, 443−449.
9. Suelter, C. H., Wang, J., and Snell, E. E. (1976) Direct Spectrophotometric Assay of Tryptophanase, *FEBS Lett. 66*, 230−232.
10. Watanabe, T., and Snell, E. E. (1977) The Interaction of *Escherichia coli* Tryptophanase with Various Amino Acids and Their Analogs. Active Site Mapping, *J. Biochem. 82*, 733−745.
11. Phillips, R. S. (1987) Reactions of O-Acyl-L-serines with Tryptophanase, Tyrosine Phenol-lyase and Tryptophan Synthase, *Arch. Biochem. Biophys. 256*, 302−310.
12. Sloan, M. S., and Phillips, R. S. (1996) Effects of α-Deuteration and of Aza and Thia Analogs of L-Tryptophan on Formation of Intermediates in the Reaction of *Escherichia coli* Tryptophan Indole-lyase, *Biochemistry 35*, 16165−16173.
13. Phillips, R. S., Sundararju, B., and Faleev, N. G. (2000) Proton Transfer and Carbon−Carbon Bond Cleavage in the Elimination of Indole Catalyzed by *Escherichia coli* Tryptophan Indole-lyase, *J. Am. Chem. Soc. 122*, 1008−1114.
14. Phillips, R. S. (1991) The Reaction of Indole and Benzimidazole with Amino Acid Complexes of *E. coli* Tryptophan Indole-lyase: Detection of a New Reaction Intermediate, *Biochemistry 30*, 5927−5934.
15. Phillips, R. S. (1989) The Mechanism of Tryptophan Indole-lyase: Insights from Pre-steady-state Kinetics and Substrate and Solvent Isotope Effects, *J. Am. Chem. Soc. 111*, 727−730.
16. Lee, M., and Phillips, R. S (1995) The Mechanism of *Escherichia coli* Tryptophan Indole-lyase: Substituent Effects on Steady-state and Pre-steady-state Kinetic Parameters for Aryl-substituted Tryptophan Derivatives, *Biol. Med. Chem. 3*, 195−205.
17. Phillips, R. S., Bender, S. L., Brzovic, P., and Dunn, M. F. (1990) The Mechanism of Binding of Substrate Analogues to Tryptophan Indole-lyase: Studies Using Rapid-Scanning and Single Wavelength Stopped-Flow Spectrophotometry, *Biochemistry 29*, 8608−8614.
18. Phillips, R. S., Johnson, N., and Kamath, A. V. (2002) Formation *in vitro* of Hybrid Dimers of H463F and Y74F Mutant *Escherichia coli* Tryptophan Indole-lyase Rescues Activity with L-Tryptophan, *Biochemistry 41*, 4012−4019.
19. Demidkina, T. V., Zakomirdina, L. N., Kulikova, V. V., Dementieva, I. S., Faleev, N. G., Gollnick, P. D., Ronda, L., Mozzarelli, A., and Phillips, R. S. (2003) The Role of Aspartate-133 and Histidine-458 in the Mechanism of Tryptophan Indole-lyase from *Proteus vulgaris*, *Biochemistry 42*, 11161−11169.
20. Dua, R. K., Taylor, E. W., and Phillips, R. S. (1993) S-Aryl-L-cysteine S,S-Dioxides: Design and Evaluation of a New Class of Mechanism Based Inhibitors of Kynureninase, *J. Am. Chem. Soc. 115*, 1264−1270.
21. Phillips, R. S., and Gollnick, P. D. (1989) Evidence that Cysteine-298 is in the Active Site of Tryptophan Indole-lyase, *J. Biol. Chem. 254*, 10627−10632.
22. Bradford, M. M. (1976) A Rapid and Sensitive Method for the Quantitation of Microgram Quantities of Protein Utilizing the Principle of Protein-dye Binding, *Anal. Biochem. 72*, 248−254.
23. Kitamura, Y., and Itoh, T. (1987) Reaction of Protonic Ionization for Buffering Agents, *J. Solution Chem. 16*, 715−725.
24. Perl, D., Holtermann, G., and Schmid, F. X. (2001) Role of the Chain Termini for the Folding Transition State of the Cold Shock Protein, *Biochemistry 40*, 15501−15511.
25. Jacob, M. H., Saudan, C., Holtermann, G., Martin, A., Perl, D., Merbach, A. E., and Schmidt, F. X. (2002) Water Contributes Actively to the Rapid Crossing of a Protein Unfolded Barrier, *J. Mol. Biol. 318*, 837−845.
26. Matheson, I. B. C. (1990) A critical comparison of least absolute deviation fitting (robust) and least-squares fitting: The importance of error distributions, *Comput. Chem. 14*, 49−57.

27. Strickland, S., Palmer, G., and Massey, V. (1975) Determination of Dissociation Constants and Specific Rate Constants of Enzyme−substrate (or Protein−ligand) Interactions from Rapid Reaction Kinetic Data, *J. Biol. Chem. 250*, 4048−4052.
28. Kiick, D. M., and Phillips, R. S. (1988) Mechanistic Deductions from Multiple Kinetic and Solvent Isotope Effects and pH Studies of Pyridoxal Phosphate-Dependent Carbon−Carbon Lyases: *Escherichia coli* Tryptophan Indole-lyase, *Biochemistry 27*, 7333−7338.
29. Sundararaju, B., Chen, H., Shillcutt, S., and Phillips, R. S. (2000) The Role of Glutamic Acid-69 in the Activation of *Citrobacter freundii* Tyrosine Phenol-lyase by Monovalent Cations, *Biochemistry 39*, 8546−8555.
30. Hogberg-Raibaud, A., Raibaud, O., and Goldberg, M. E. (1975) Kinetic and equilibrium studies on the activation of *Escherichia coli* K12 tryptophanase by pyridoxal 5′-phosphate and monovalent cations, *J. Biol. Chem. 250*, 3352−3358.
31. Suelter, C. H., and Snell, E. E. (1977) Monovalent cation activation of tryptophanase, *J. Biol. Chem. 252*, 1852−1857.
32. Isaacs, N. S. (1984) The Effects of Pressure on Kinetic Isotope Effects, in *Isotopes in Organic Chemistry* (Buncel, E., and Lee, C. C., Eds.) Vol. 6, pp 67−105, Elsevier, Amsterdam.
33. Grant, K. L., and Klinman, J. P. (1989) Evidence that both Protium and Deuterium undergo Significant Tunneling in the Reaction Catalyzed by Bovine Serum Amine Oxidase, *Biochemistry 28*, 6597−6605.
34. Bahnson, B. J., Park, D. H., Kim, K., Plapp, B. V., and Klinman, J. P. (1993) Unmasking of Hydrogen Tunneling in the Horse Liver Alcohol Dehydrogenase Reaction by Site-directed Mutagenesis, *Biochemistry 32*, 5503−5507.
35. Sikorski, R. S., Wang, L., Markham, K. A., Rajagopalan, P. T., Benkovic, S. J., and Kohen A. (2004) Tunneling and Coupled Motion in the *Escherichia coli* Dihydrofolate Reductase Catalysis, *J. Am. Chem. Soc. 126*, 4778−4779.
36. Rickert, K. W., and Klinman, J. P. (1999) Nature of Hydrogen Transfer in Soybean Lipoxygenase 1: Separation of Primary and Secondary Isotope Effects, *Biochemistry 38*, 12218−12228.
37. Cook, P. F., Tai, C. H., Hwang, C. C., Woehl, E. U., Dunn, M. F., and Schnackerz, K. D. (1996) Substitution of pyridoxal 5′-phosphate in the *O*-acetylserine sulfhydrylase from *Salmonella typhimurium* by cofactor analogs provides a test of the mechanism proposed for formation of the α-aminoacrylate intermediate, *J. Biol. Chem. 271*, 25842−25849.
38. Isaacs, N. S., Javaid, K., and Rannala, E. (1977) Pressure effects on proton tunneling, *Nature 268*, 372.
39. Isaacs, N. S. (1995) *Physical Organic Chemistry*, 2nd ed., p 306, Longman, Singapore.
40. Northrop, D. B., and Cho, Y. K. (2000) Effect of Pressure on Deuterium Isotope Effects of Yeast Alcohol Dehydrogenase: Evidence for Mechanical Models of Catalysis, *Biochemistry 39*, 2406−2412.
41. Park, H., Kidman, G., and Northrop, D. B. (2005) Effects of Pressure on Deuterium Isotope Effects of Yeast Alcohol Dehydrogenase using Alternative Substrates, *Arch. Biochem. Biophys. 433*, 335−340.
42. Quirk, D. J., and Northrop, D. B. (2001) Effect of Pressure on Deuterium Isotope Effects of Formate Dehydrogenase, *Biochemistry 40*, 847−851.

BI051062A